

Scientific Article

Measurement and Incorporation of Laryngeal Motion Using cine-MRI on an MR-Linear Accelerator to Generate Radiation Therapy Plans for Early-stage Squamous Cell Cancers of the Glottis



Amit Gupta, MBBS, MRCP, FRCR,^{a,*} Dualta McQuaid, PhD, MSc, MSci,^b Alex Dunlop, PhD,^b Helen Barnes, BSc(Hons),^c Jonathan Mohajer, MSc,^b Gillian Smith,^c Jayde Nartey,^c Kian Morrison,^c Trina Herbert,^c Sophie Alexander, MSc,^a Helen McNair, PhD,^a Kate Newbold, MB ChB, MRCP, FRCR, MD(Res), FRCP(E),^c Chris Nutting, BSc, MBBS, FRCP, FRCR, MD, PhD, PIPEM, FRSB, FInst,^a Shreerang Bhide, MBBS, MRCP, FRCR, PhD,^a Kevin Joseph Harrington, MBBS, PhD, FRCP, FRCR,^{a,1} and Kee Howe Wong, MBBS, FRCR, MD(Res)^{c,1}

^aThe Royal Marsden NHS Foundation Trust and The Institute of Cancer Research, Head & Neck Unit, London, United Kingdom; ^bThe Joint Department of Physics, The Royal Marsden Hospital and The Institute of Cancer Research, Sutton, United Kingdom; and ^cThe Royal Marsden NHS Foundation Trust, Sutton, United Kingdom

Received 19 October 2023; accepted 26 February 2024

Purpose: Swallow-related motion of the larynx is most significant in the cranio-caudal directions and of short duration. Conventional target definition for radical radiation therapy includes coverage of the whole larynx. This study longitudinally examined respiration- and swallow-related laryngeal motions using cine-magnetic resonance imaging. We further analyzed the dosimetry to organs at risk by comparing 3D-conformal radiation therapy (3D-CRT), volumetric modulated arc therapy (VMAT), and intensity modulated radiation therapy (IMRT) techniques.

Methods: Fifteen patients with T1-2 N0 glottic squamous cell carcinomas were prospectively recruited for up to 3 cine-MRI scans on the Elekta Unity MR-Linear accelerator, at the beginning, middle, and end of a course of radical radiation therapy. Swallow frequency and motion of the hyoid bone, cricoid and thyroid cartilages, and vocal cords were recorded during swallow and rest. Adapted treatment volumes consisted of gross tumor volume + 0.5-1 cm to a clinical target volume with an additional internal target volume (ITV) for personalized resting-motion. Swallow-related motion was deemed infrequent and was not accounted for in the ITV. We compared radiation therapy plans for 3D-CRT (whole larynx), VMAT (whole larynx), and VMAT and IMRT (ITV for resting motion).

Sources of support: This work was supported by the Cancer Research UK programme grants C7224/A13407, C33589/A19727, and C33589/A28284. Research data are not available at this time.

¹K.J.H. and K.H.W. are both joint senior authors.

*Corresponding author: Amit Gupta, MBBS; Email: amit.gupta9@nhs.net

<https://doi.org/10.1016/j.adro.2024.101490>

2452-1094/Crown Copyright © 2024 Published by Elsevier Inc. on behalf of American Society for Radiation Oncology. This is an open access article under the CC BY-NC-ND license (<http://creativecommons.org/licenses/by-nc-nd/4.0/>).

Results: Resting- and swallow-related motions were most prominent in the cranio-caudal plane. There were no significant changes in the magnitude of motion over the course of radiation therapy. There was a trend of a progressive reduction in the frequency of swallow. Treatment of partial larynx volumes with intensity modulated methods significantly reduced the dose to carotid arteries, compared with treatment of whole larynx volumes. Robustness analysis demonstrated that when accounting for intrafraction swallow, the total dose delivered to the ITV/planning target volume was maintained at above 95%.

Conclusions: Swallow-related motions are infrequent and accounting for resting motion in an ITV is sufficient. VMAT/IMRT techniques that treat more conformal targets can significantly spare critical organs at risk such as the carotid arteries and thyroid gland, potentially reducing the risk of carotid artery stenosis-related complications and other long-term complications.

Crown Copyright © 2024 Published by Elsevier Inc. on behalf of American Society for Radiation Oncology. This is an open access article under the CC BY-NC-ND license (<http://creativecommons.org/licenses/by-nc-nd/4.0/>).

Introduction

Treatment of early-stage glottic squamous cell carcinomas (ESGC; T1-2, N0) in the United Kingdom conventionally involves irradiation of the whole larynx. The clinical target volume (CTV) is typically defined from the inferior edge of the hyoid to the inferior edge of the cricoid cartilage to cover tumor motion during deglutition and potential microscopic disease within the supra-/sub-glottic regions. Traditionally, 3D-conformal radiation therapy (3D-CRT) with a lateral parallel-opposed beam arrangement is used. More recently, the majority of centers have adopted the intensity modulated radiation therapy (IMRT) technique.

A recent randomized controlled trial comparing transoral laser surgery against 3D-CRT for T1a ESGC showed comparable overall and disease-specific survival and laryngeal preservation rates between the 2 strategies.¹ Therefore, there is interest in shifting toward smaller target delineations to treat tissue volumes, similar to laser microsurgery. This may be achieved through exclusion of swallow-related motion and may result in reduced irradiation of organs at risk (OARs).

The larynx is not a fixed structure, as its components move independently of surrounding soft tissues. The aim of this study was three-fold: (a) to investigate the resting- and swallow-related motions of the hyoid bone and laryngeal structures using cine-magnetic resonance imaging (cine-MRI), (b) to assess the evolution of motion-related changes during a patient's course of radiation therapy, and (c) to conduct a radiation therapy planning study based on motion data to generate individualized treatment volumes and evaluate the dosimetric impact on OARs, compared with that associated with conventional radiation therapy volumes.

Methods and Materials

Patient selection

Patients with ESGC receiving radical hypofractionated radiation therapy, 55 Gy in 20 fractions over 4 weeks,

were recruited into PRIMER (NCT02973828) and MOMENTUM (NCT04075305). These studies received approval from institutional clinical research boards and research committee boards. Patients consented to up to 3 cine-MRI sessions on the Elekta Unity MR-Linear accelerator (MR-Linac) (Elekta AB, Stockholm, Sweden) at the beginning (fractions 1-4), middle (fractions 9-11), and end (fractions 16-20) of radiation therapy. All patients were positioned supine with arms down and immobilized in a neutral neck position with a 5-point thermoplastic head shell. A shoulder wedge was used if required to assist with neck positioning.

Image acquisition and analysis

Cine-MRI

All cine-MRIs were performed on the Philips (Best, the Netherlands) 1.5 T MRI scanner, part of the MR-Linac with a standardized head and neck receiver coil (flip angle, 35°; echo time/repetition time, 2.298/4.577 ms; matrix, 120; bandwidth, 479 Hz; number of signal averages, 1; pixel spacing, 0.8 × 0.8 mm; frames per second, 4).

Cine-MRI captured motion in the axial (level of vocal cords), coronal (view of both cricoid and thyroid cartilages), and sagittal (between vocal cords) planes for 3 min. Consistency of scanning positions for each patient was achieved by providing radiographers with labeled printouts to aid localization. Each scan session consisted of 2 min of scanning at rest (where the patient was free to swallow at their natural rate) and 1 min of active swallowing every 10 to 15 s (to ensure that a minimum of 3 swallow events were captured).

Motion analysis

Quality assurance of the MRI scanner, including image-distortion analysis of Elekta-approved sequences, was performed using the Philips MR distortion phantom, as recommended by the manufacturer.² Prior in-house analyses of cine-MRIs using methods described by Riis et al demonstrated no geometric or anatomic distortions after importing the DICOMs into the RayStation treatment planning system (TPS; V10.0.1.52, RaySearch Laboratories AB, Sweden).³

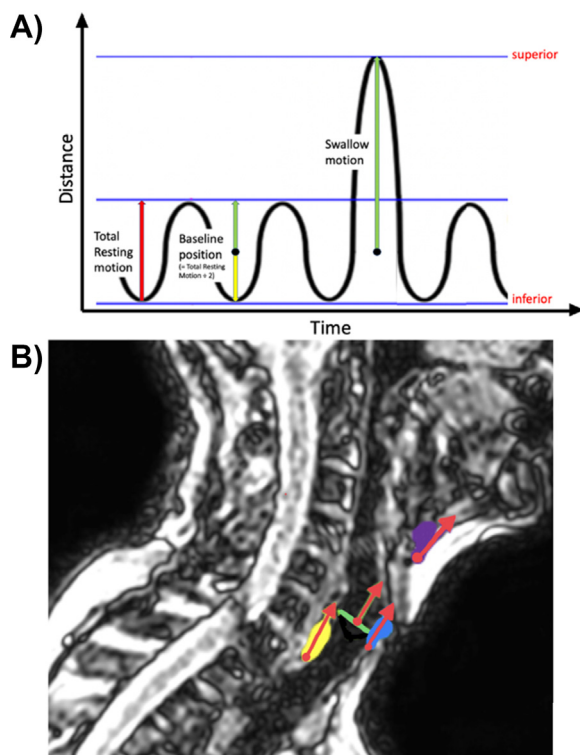


Figure 1 Definition of motion measurements. (A) Respiratory-related motions were recorded from the inferior- to superior-most positions. This distance was halved and designated the baseline position. Swallow distances were also measured from the inferior-most positions of each structure; however, half the resting distance was subtracted to determine swallow motion from the baseline position. (B) Sagittal cine-magnetic resonance imaging slice depicts cricoid cartilage (yellow), thyroid cartilage (blue), hyoid bone (purple), and vocal cord level (green). Arrows (red) denote the points at which measurements were taken.

Motions of the vocal cords, hyoid bone, and cricoid and thyroid cartilages were measured in the cranio-caudal directions. The gross tumor was not well visualized on cine-MRI, and it was assumed that for T1-2 ESGC, vocal cord motion would be an appropriate surrogate for the primary tumor, because by definition, there is no fixation of the vocal cord. The edges of each structure were used to measure motion, because they were the most visible features. Cranio-caudal motion was measured from the most inferior to the most superior position (Fig. 1). Owing to the respiration-related tidal-wave motion of the larynx, this distance was halved to estimate the baseline position of each laryngeal substructure. It was from this baseline position that the maximal swallow distance was recorded.

Thyroid cartilage has a rotational component during swallow because of the anterior pull on the superior notch of the cartilage by the thyro-hyoid ligament. Therefore, the superior and inferior points of the thyroid cartilage were measured independently. Left-right motion of both

vocal cords and carotid arteries were measured on the axial image sets. Patients' vertebral alignments were not always parallel to the treatment couch. Motion distances in RayStation would reflect superior-inferior motion along the plane of the couch rather than the true anatomic motion along the plane of the vertebrae. Therefore, actual spatial motions were captured to include any anterior components. All measurements were reported as the mean of triplicate recordings.

Duration of swallow

The cricoid cartilage was the clearest structure on the cine-MRIs and was chosen as the surrogate for measuring duration of swallow. The starting position for swallow was defined as the position of the cricoid cartilage during rest. End of swallow was defined as the return of the cricoid cartilage to its starting position. The excursion time of the cricoid was measured in number of frames (0.25 s per frame).

Radiation therapy planning studies

A noncontrast-enhanced planning computed tomography (CT) scan from the vertex to carina was taken in 2 mm slices and with a 1×1 mm pixel size. All patients received radical radiation therapy using 3D-CRT plans designed by a physicist.

Three additional plans were created for each patient by a clinical oncologist with oversight from a senior physicist (Fig. 2). A nonadapted volumetric modulated arc therapy (VMAT) plan, termed "VMAT_NA", was created to treat the whole larynx. Motion data analyses revealed infrequent swallow events that were not accounted for in subsequent planning studies. Therefore, resting motion data were used to formulate individual-level internal target volumes (ITVs). Resting motion of the cricoid cartilage was chosen for the ITV because this structure had the most consistent visibility on cine-MRI. Motion-adapted volume VMAT plans ("VMAT_A") were created on RayStation to simulate treatment on a C-arm linear accelerator, and IMRT plans ("IMRT_A"), on the Monaco TPS (V 5.59.02, Elekta AB, Stockholm, Sweden), to simulate treatment on the MR-Linac. The dose fractionation was 55 Gy in 20 fractions over 4 weeks.

Target definitions and planning parameters/constraints are described in Table 1. It was deemed that a mean dose to the carotid arteries below 35 Gy was significant to reduce tunica intima-media thickness.⁴ The inferior pharyngeal-constrictor muscle (IPCM) volume intersecting with the planning target volume (PTV) was subtracted from the IPCM volume to create a "Plan_IPCM", which was used for optimization in the VMAT_NA, VMAT_A, and IMRT_A plans. A Plan_IPCM constraint of a maximum mean dose of 47 Gy was based on the "Dysphagia-Aspiration Related

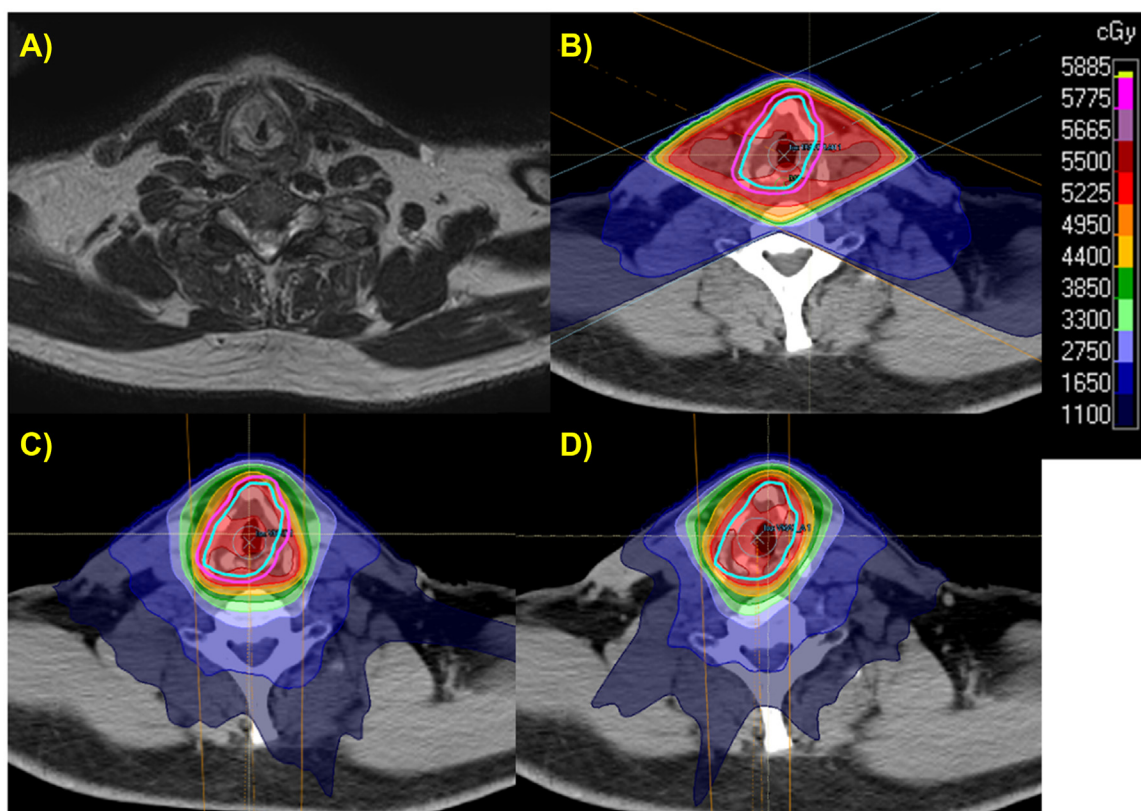


Figure 2 Example of radiation therapy plans. (A) Single axial T2-weighted magnetic resonance image at the level of the glottis, showing a T2 early-stage glottic squamous cell carcinoma involving the right vocal cord. (B) 3-Dimensional conformal radiation therapy. (C) Volumetric modulated arc therapy nonadapted plans and (D) volumetric modulated arc therapy-adapted plans demonstrate the differences in dosimetry at the same levels for this patient. Displayed are the internal target volumes (cyan) and planning target volumes (magenta).

Structures” study (D_{mean} , 50 Gy), adjusted for the higher dose per fraction of 2.75 Gy and alpha:beta ratio of 10 for acute toxicities.⁵ The final mean dose was reported for the complete IPCM structure.

3D-CRT plans

Plans were created with 6 MV parallel-opposed fields or anterior-oblique fields. A soft-tissue equivalent bolus (0.5-1 cm) was used for cases with anterior commissure involvement if superficial dose coverage was poor. The dose was prescribed to the International Commission on Radiation Units and Measurements reference point, which was typically at the isocenter, placed in the center of the PTV. There were no dose objectives or constraints for any OARs for this planning technique, as per institutional standard clinical practice.

VMAT plans

VMAT plans were produced using a collapsed-cone algorithm (V5.6) on the RayStation TPS. Plan parameters included a single-beam full arc (360°) using 6 MV flattening-filter-free photons, with a gantry spacing of 2°, 40

maximum optimization iterations, and a dose-grid resolution of 0.25 cm³. The dose was scaled and prescribed to the median (50%) of the PTV.

IMRT plans

IMRT_A plans were created on Monaco, using a Monte Carlo dose engine. Treatment plans consisted of 9-field step-and-shoot IMRT utilizing 7 MV flattening-filter-free photons (beam angles, 145°, 95°, 65°, 30°, 0°, 330°, 295°, 265°, and 215°). There were 60 maximum segments per beam; minimum segment width, area, and monitor units of 0.5 cm, 4 cm², and 6, respectively; and medium fluence smoothing. Plans were calculated with dose uncertainties of 2% per plan and a dose-grid resolution of 3 mm, with dose prescriptions to 50% of the PTV.

Impact of swallow on target dosimetry

Individual-level data on swallow distance, frequency, and duration; monitor units delivered per minute; total fraction delivery time; and dosimetry data for 3D-CRT, VMAT_NA, VMAT_A, and IMRT_A were acquired. The point of maximal displacement of the superior and

Table 1 Radiation therapy planning target definitions

| (A) 3D-CRT/VMAT (VMAT_NA) (conventional volumes) | | |
|--|--|-------------------------|
| Structure | Recipe | Notes |
| CTV | Whole larynx | |
| PTV | CTV + isotropic 3 mm isotropic | |
| IPCM | Inferior hyoid to superior cricoid cartilages | For dose reporting only |
| Plan_IPCM | IPCM minus PTV | |
| Thyroid | Whole thyroid gland | |
| Thyroid PRV | Thyroid gland + 3 mm | For dose reporting only |
| Spinal cord | 2 cm superior and inferior to PTV | |
| Spinal cord PRV | Spinal cord + 3 mm | |
| Ipsilateral & contralateral carotid arteries (separate ROIs) | 1 cm superior and inferior to PTV | For dose reporting only |
| Ipsilateral & contralateral carotid artery PRV | Ipsilateral & contralateral carotid arteries + 3 mm | |
| (B) VMAT (VMAT_A)/IMRT (IMRT_A) (adapted volumes) | | |
| Structure | Recipe | Notes |
| GTV | - Involved vocal cord for T1a/b - Full tumor extent for T2 | |
| CTV | GTV + 0.5 cm (T1)/1 cm (T2) | |
| ITV | CTV + respiratory-related motion (grown in inferior, superior and anterior directions) | |
| PTV | (CTV + ITV) + isotropic 3 mm | |
| IPCM | Inferior hyoid to superior cricoid cartilages | For dose reporting only |
| Plan_IPCM | IPCM minus PTV | |
| Thyroid | Whole thyroid gland | |
| Thyroid PRV | Thyroid gland + 3 mm | For dose reporting only |
| Spinal cord | 2 cm superior and inferior to PTV | |
| Spinal cord PRV | Spinal cord + 3 mm | |
| Ipsilateral & contralateral carotid arteries (separate ROIs) | 1 cm superior and inferior to PTV | |
| Ipsilateral & contralateral carotid artery PRV | Ipsilateral & contralateral carotid arteries + 3 mm | |
| (C) Planning Optimization Objectives (for VMAT_NA, VMAT_A and IMRT_A plans) | | |
| Structure | Recipe | |
| PTV | Dose (minimum): 53.9 Gy Dose (maximum): 56.1 Gy Uniform dose: 55 Gy Volume receiving 54.85 Gy: ≥ 50% Volume receiving 55.15 Gy: ≤ 50% Dose to 95% of the PTV: ≥ 52.25 Gy Target equivalent uniform dose: 55 Gy | |
| Spinal cord | Dose (maximum): 25 Gy to 0.10 cm ³ | |
| Spinal cord PRV | Dose (maximum): 30 Gy to 0.10 cm ³ | |
| Ipsilateral & contralateral carotid artery PRVs | Dose (maximum): 35 Gy to 0.10 cm ³ Dose to 50% of the volume: < 10 Gy | |
| Plan IPCM | Dose (mean): < 47 Gy | |
| <p>(A) Volumes for conventional volumes, planned using either 3-dimensional conformal radiation therapy or volumetric modulated arc therapy techniques. (B) Volumes for adapted volumes, planned using either volumetric modulated arc therapy or intensity modulated radiation therapy techniques. (C) Planning objectives were kept the same for all non-3-dimensional conformal radiation therapy modalities. However, VMAT_NA, VMAT_A, and IMRT_A plans were optimized to the “Plan_IPCM” structure.</p> <p><i>Abbreviations:</i> 3D-CRT = 3-dimensional conformal radiation therapy; CTV = clinical target volume; EUD = equivalent uniform dose; GTV = gross tumor volume; IMRT = intensity modulated radiation therapy; IPCM = inferior pharyngeal-constrictor muscle; ITV = internal target volume; PRV = planning risk volume; PTV = planning target volume; ROI = region of interest; VMAT = volumetric modulated arc therapy.</p> | | |

anterior apex of the ITV/PTV during swallow was determined by using individual cranio-caudal and anterior-posterior swallow distance data. Based on all this information, the percentage dose received by the ITV/PTV edge for the duration of swallow was calculated. It was assumed that the baseline swallow frequency was maintained for the whole treatment course, simulating the worst-case scenario.

Statistical analysis

To assess for differences in motion between the start and end of radiation therapy, paired motion data were compared using a Wilcoxon signed rank-sum test. The Wilcoxon signed rank-sum test was also used to assess the significance of any differences in the dosimetry between the planning modalities. The significance threshold was set at $P < .05$.

Results

Laryngeal motion study

Fifteen patients were prospectively recruited for laryngeal motion analyses. Seven patients had T1 ESGC (T1a = 6 and T1b = 1), and 7 patients had T2 ESGC. One patient had metastatic laryngeal squamous cell carcinoma, with a single mediastinal node only. This patient was recruited for motion capture only and excluded from the radiation therapy-planning phase. Eleven patients were male, and 3 were female. Seven patients had all 3 serial cine-MRIs, 5 patients had 2, and 3 patients had 1.

Tables 2A and B display the motion data from the different laryngeal components at rest and during swallow, respectively. Figure 3A displays the swallow-related motion data. The greatest extent of motion was in the cranio-caudal plane (20.2-24.8 mm). The mean cranio-caudal motion of the hyoid cartilage was 17.1 mm. The differences in swallow-related motions between the beginning and end of radiation therapy were significant in the left-right directions for the ipsilateral and contralateral carotid arteries only ($P < .05$).

Motions of the superior (mean, 20.6 mm; standard deviation (SD), 2.2 mm) and inferior (mean, 21.2 mm; SD, 1.7 mm) components of the thyroid and cricoid (mean, 22.7 mm; SD, 0.7 mm) cartilages were predominantly in the cranial direction (Fig. 3B). However, there was an anterior component of motion in all of these structures (grouped mean, 6.6 mm; SD, 1.5 mm). The hyoid bone had greater anterior motion (mean, 9.9 mm; SD, 1.2 mm) than the laryngeal structures.

A trend of a decreasing number of swallows per minute was noted ($P = .10$) (Table 2C). The maximum mean

rate of swallow across all patients was 1 per minute (SD, 1). The mean duration of each swallow event was 1.5 s (SD, 0.4 s) with no significant change during radiation therapy ($P = .89$).

Motion-based radiation therapy planning

Fourteen patients with ESGC had radiation therapy plans generated. 3D-CRT and VMAT_NA failed bilateral carotid artery (V35/V10) and IPCM constraints. VMAT_A was the best performing modality, with a single failure of the ipsilateral carotid artery V10. IMRT_A failed both ipsilateral and contralateral carotid artery V10 constraints.

Whole larynx volumes planned with either 3D-CRT or VMAT_NA delivered significantly higher mean doses to the ipsilateral and contralateral carotid arteries (Fig. 4A and 4B). Detailed dosimetry data for the PTV and OARs are displayed in Appendix A. IMRT_A delivered a significantly lower mean dose to the ipsilateral carotid artery (V35, 34.0 Gy, and V10, 15.8 Gy) in T2-stage tumors, compared with VMAT_A (V35, 35.0 Gy, and V10, 23.8 Gy) ($P < .05$). Conversely, VMAT_A delivered significantly lower doses to the contralateral carotid arteries in both T1- and T2-stage tumors ($P < .05$).

Mean maximum spinal cord doses were significantly higher with the VMAT/IMRT techniques, and 3D-CRT delivered the lowest maximum spinal cord dose in T1 (3.7 Gy) or T2 (10.1 Gy) tumors. VMAT_A delivered the lowest maximum spinal cord dose out of the intensity modulated methods for T1 (21.3 Gy) and T2 (23.0 Gy) tumors.

VMAT_A and IMRT_A significantly improved IPCM doses, with VMAT_A superior to IMRT_A in T1-stage tumors only (35.9 vs 45.0 Gy, respectively) ($P < .05$). There was mild sparing of contralateral arytenoids and vocal cords from adapted volumes, with small but significant differences in the mean doses between VMAT_NA and VMAT_A/IMRT_A.

The mean dose to the thyroid glands was significantly lower with VMAT/IMRT techniques compared with 3D-CRT, with further significant sparing of the thyroid gland with adapted volumes compared with VMAT_NA, for both T1 and T2 tumors.

Impact of swallowing on dose delivery

When accounting for any swallow-related motion for each patient, a mean ITV dose of >52.25 Gy (95%) was achieved for VMAT_NA (54.3 Gy; SD, 0.8), VMAT_A (53.9 Gy; SD, 1.1), and IMRT_A (54.3 Gy; SD, 1.3). Only a single patient with a T2-stage tumor would have received 94.7% of the dose to the ITV with VMAT_A when accounting for swallow. The mean PTV doses remained at >52.25 Gy with VMAT_NA (53.8 Gy; SD, 1.1) and VMAT_A (54.2 Gy; SD, 1.3).

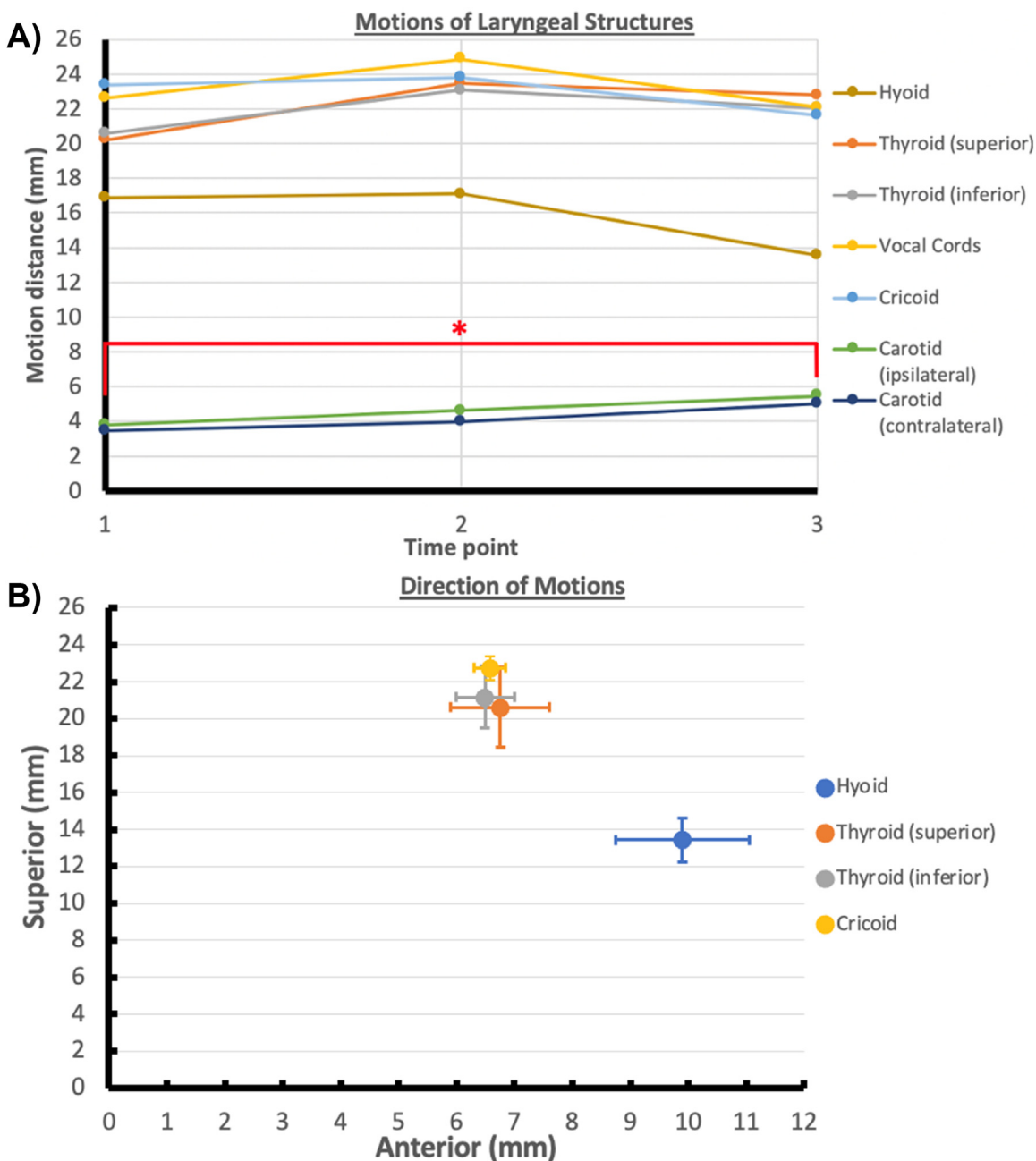


Figure 3 Mean swallow-related motion data. (A) Swallow-related motion for laryngeal sub-structures, hyoid cartilage, and both carotid arteries are shown. Motion for carotid arteries was measured in the left-right directions, and motion for all other structures was measured in the cranio-caudal directions. Standard deviations for the mean measurements are reported in Table 2B. *Differences in the motion of both carotid arteries were significant between the start and end of radiotherapy ($P < .05$). (B) Motion of laryngeal subcomponents and hyoid cartilage is separated into cranial and anterior elements to demonstrate the variations in patient setup and highlight the lack of perpendicular vertebral alignment with the treatment couch. Error bars denote single standard deviations.

Table 2 Laryngeal motion (mm), duration, and frequency data

| (A) Structure | REST: Time point | | |
|---|---------------------|------------|------------|
| | 1 (n = 15) | 2 (n = 11) | 3 (n = 9) |
| Hyoid | 1.8 (0.9) | 1.5 (1.4) | 1.4 (1.0) |
| Thyroid | 3.0 (2.4) | 3.1 (1.7) | 3.0 (2.3) |
| Cricoid | 3.0 (2.4) | 3.2 (2.3) | 3.3 (2.3) |
| Vocal cords (cranio-caudal) | 2.8 (2.4) | 2.9 (2.1) | 2.8 (2.8) |
| Vocal cord (ipsilateral, left-right) | 1.8 (1.2) | 1.7 (1.1) | 1.6 (0.8) |
| Vocal cord (contralateral, left-right) | 1.8 (0.6) | 1.5 (1.0) | 1.4 (0.6) |
| (B) Structure | SWALLOW: Time point | | |
| | 1 (n = 15) | 2 (n = 11) | 3 (n = 9) |
| Hyoid | 16.9 (4.4) | 17.1 (4.6) | 13.6 (7.9) |
| Thyroid (superior notch) | 20.2 (7.1) | 23.4 (5.7) | 22.8 (3.3) |
| Thyroid (inferior notch) | 20.6 (5.5) | 23.1 (5.5) | 22.1 (3.8) |
| Cricoid | 23.4 (5.9) | 23.8 (5) | 21.6 (4.8) |
| Vocal cords (cranio-caudal) | 22.6 (5.3) | 24.8 (5.1) | 22.1 (3.4) |
| Carotid artery (ipsilateral, left-right) | 3.8 (2.5) | 4.6 (3.6) | 5.4 (3.6) |
| Carotid artery (contralateral, left-right)) | 3.4 (2.3) | 4.0 (2.7) | 5.0 (2.0) |
| (C) | Time point | | |
| | 1 (n = 15) | 2 (n = 11) | 3 (n = 9) |
| Mean number of swallows per minute (SD) | 1 (1) | 0.6 (0.8) | 0.3 (0.4) |
| Mean duration of swallows (s, SD) | 1.5 (0.3) | 1.5 (0.4) | 1.5 (0.3) |

Data are shown for laryngeal substructure motions (A) at rest and (B) during swallow at 3 time points spread over the course of patients' radiation therapies. All measurements are displayed in millimeters with standard deviations in parentheses, rounded to single decimal places. Unless stated otherwise, all measurements represent cranio-caudal motions for each structure. The mean numbers and durations of swallows across all patients are shown in (C).

Abbreviations: SD = standard deviation.

Discussion

Motion and toxicity analyses

The data reported in this study show that cine-MRI can detect respiration-related motions of the larynx, hyoid bone, and carotid arteries in all anatomic planes. Prior studies of laryngeal motion have utilized a variety of modalities such as videofluoroscopy,^{6,7} megavoltage/kilovoltage photons,⁸ and MRI.^{9,10} Bradley et al analyzed the motion of tumors from a range of head and neck subsites, only 5 of which were glottic cancers.⁹ Bradley et al and Gurney-Champion et al used MRI sequences that had longer image acquisition times, which required postprocessing to extract the motion data.¹⁰ This led to the potential missing of minute fluctuations in motion and image registration errors.

Bruijnen et al employed cine-MRI to explore swallowing and resting motion in a variety of head and neck cancers, including 29 laryngeal cancers. They showed that the mean resting cranio-caudal motion of the larynx is up to 3.8 mm.¹¹ Osman et al used 4D-CT to focus on vocal

cord motion as part of their workup toward single vocal cord irradiation and demonstrated limited vocal cord motion at rest.¹²

Although other institutions have demonstrated the utility of cine-MRI-based motion assessments on the MR-Linac for abdominal tumors,^{13,14} there are no published data on MR-Linac assessments of laryngeal motion in multiple subjects. The magnitudes of motion in this study are consistent with those in the literature. The strength of this study lies in its homogeneity compared with other MRI-based studies.

Variations in motion between patients resulted in insignificant differences, seen in degrees of motion of all laryngeal structures and the hyoid bone. CT-based 3D reconstruction of the thyroid cartilage identified significant effects of sex, age, and body mass index on its size and angulation,¹⁵ which correlate with the length of the thyro-arytenoid muscle.¹⁶ Respiratory and swallow dynamics have also been noted to change over the course of a lifespan, collectively providing potential explanations for the variability in motion observed in our study.¹⁷

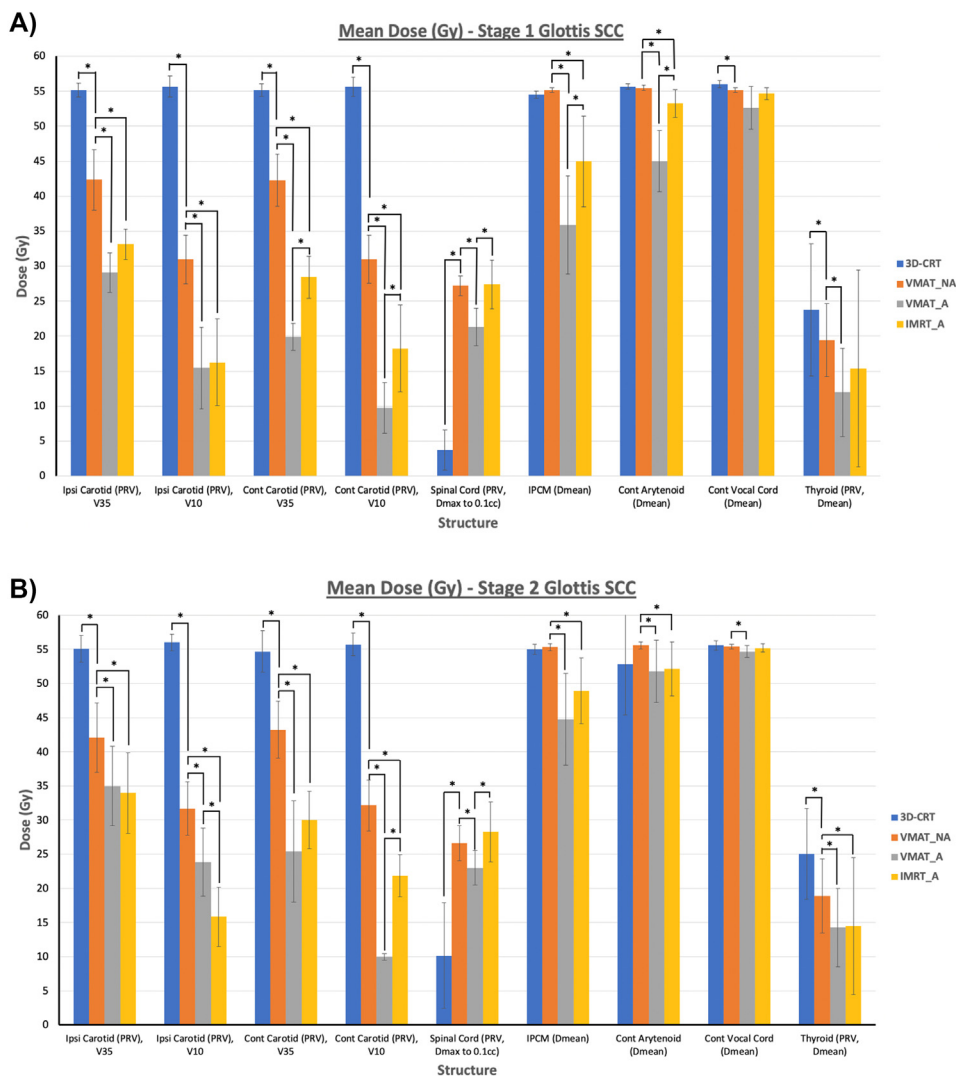


Figure 4 Mean doses for organs at risk. Mean doses for (A) Stage 1 (T1) and (B) Stage 2 (T2) squamous cell carcinomas of the glottis are graphed with single standard deviations. *Significant difference ($P < .05$). Abbreviations: Cont/ Ipsi = contralateral/ipsilateral; IPCM = inferior pharyngeal constrictor muscle; PRV = planning risk volume.

Van Asselen et al showed that the frequency of swallow is highest in the first 5 fractions of radiation therapy, after which the frequency is reduced in mid-treatment, which is a similar finding to our data.⁸ Bahig et al reported no differences in the magnitudes of whole larynx motion between the beginning and middle of treatment, but the anatomic part of the larynx used to measure swallow was not described.¹⁸

In the respiratory cycle, exhalation is a longer event than inspiration, with a relative ratio of 2-3:1.¹⁹ Therefore, it would be expected that the larynx is mostly located in the inferior-most position during rest. It was assumed that swallowing would start from a position at the midpoint between full expiration and inspiration. For this reason, resting motion data are reported as maximal motions of the structures at rest, whereas swallowing data are

recorded as maximal motion from the point of maximal exhalation, with half the respiration motion subtracted from the final value. Therefore, all motion data were interpreted and reported in the cranial direction only.

It is not standard practice at our institute to instruct patients to avoid swallow or maintain maximal exhalation during CT acquisition, although this approach has been reported to be feasible.^{10,12,20} Therefore, patients may have had their planning CTs acquired during inspiration or swallowing, which does not fully reflect the ideal clinical scenario. Thus, the planning data shown in this study reflect a proof-of-principle to demonstrate that adapted radiation therapy volumes are feasible.

This work was performed on the MR-Linac with a view to further developing image-guided radiation therapy and gating to minimize the treatment volume. However,

institutions without an MR-Linac may have MRI scanners, where the diagnostic clinical workload may preclude their uses for cine-MRI. Some diagnostic MRIs do not have the necessary equipment to immobilize and position patients for radiation therapy. These factors may prevent the use of cine-MRI for this purpose.

Planning studies

The planning studies demonstrated improved dosimetry to OARs when irradiating a smaller target with adapted volumes. Whole larynx target volumes failed a similar number of dose constraints, but VMAT_NA still significantly reduced the dose to both carotid arteries. Adapted volume performances (VMAT_A and IMRT_A) were superior to nonadapted volume performances, with more consistently satisfied dose objectives. Fixed-field IMRT leaves less room for dose conformality than VMAT and explains the more frequently failed contralateral carotid artery V10 dose constraint. However, this could be mitigated by the addition of more beam angles and by further improving the optimization strategy. The majority of volumes abutted or overlapped the ipsilateral carotid artery planning risk volumes (PRVs), and it was not possible to optimally reduce the ipsilateral carotid artery exposure without compromising PTV coverage.

The addition of further beams or segments comes at the major cost of increased fraction delivery time. Estimated mean fraction delivery times with IMRT_A plans were longer (167 s; SD, 34) than those with VMAT_A (103 s; SD, 4.8). However, this may be a compromise that is tolerable for patients, as patients with other head and neck cancers receiving treatment on the MR-Linac are known to be maintained in treatment positions for up to 85 min per fraction.^{21,22}

All non-3D-CRT plans delivered higher doses to the spinal cord, owing to a low dose bath. However, all plans maintained the set dose constraint of a maximum 30 Gy to the PRV structure. Data on normal tissue tolerances published by Emami are still regarded as the gold standard for reference.²³ Spinal cord tolerance is reported as 50 Gy in 2 Gy per fraction with a <1% rate of grade ≥ 2 myelopathy. The mean EQD2 doses to the spinal cord PRV delivered by VMAT_NA, VMAT_A, and IMRT_A were 22.5, 17.2, and 23.6 Gy, respectively. These doses confer a negligible risk of developing myelopathy and do not preclude future reirradiation in the head and neck, if required.

Swallow-related motions were deemed clinically insignificant based on the trend of a decreasing frequency of swallow and the short time per swallow event. This study demonstrates that despite the maximal frequency of swallow per patient, swallowing activity did not compromise dose delivery to the ITV/PTV target, as over 95% of the prescribed dose treated the superior edge of the target.

This is a “worst-case” estimate, as the superior edge of the target would not spend the entire duration of swallow at the maximal excursion point. Hamlet et al demonstrated the delivery of 99.49% of the dose when using 3D-CRT techniques,⁷ but there are limited studies that report the impact of swallowing when utilizing nongated/tracked treatment techniques or analyze dosimetry to smaller treatment volumes.

The work in this study was performed on both the C-arm and MR-Linac platforms. The Elekta Unity MR-Linac allows cine-MR images to be taken during beam-on time, which allows a live feed of the target position. The long-term goals of this work would be to shift toward a further reduction of the irradiated volume by eliminating the ITV and to aim for treatment of volumes more typical of laser microsurgery.

Tracking/gating systems on the 0.35T ViewRay MRIdian MR-Linac have allowed accurate and consistent treatment of mobile abdominal lesions without ITV margins, with further applications of this technique being investigated for fiducial-free stereotactic radiation therapy.^{13,24} Furthermore, online-adapted radiation therapy using the MRIdian MR-Linac has demonstrated comparable dosimetry, and in some cases, benefits to OAR doses, in a range of other primary tumor sites such as the pelvis and lung.²⁵ Huynh et al described their workflow for stereotactic radiation therapy for laryngeal cancer in a single healthy volunteer using the ViewRay MRIdian platform and demonstrated the feasibility of sufficient dose delivery to a tracked and gated target using cine-MR.²⁶ The accuracy of the ViewRay system for tracking geometric targets in phantom studies is reported to be 1.2 mm.²⁷ Tracking systems on the Elekta Unity platform were officially implemented in October 2022, but before this, they had been designed as in-house projects within other institutions.²⁸ It is envisaged that Elekta-approved tracking/gating systems may offer similarly accurate and live feedback on target positions, facilitating the delivery of treatments to ITV-free and more limited PTV targets.

Conclusion

We demonstrated that swallow-related motion can be measured using cine-MRI on the Elekta Unity MR-Linac. Swallow-related motion is infrequent, and accounting for resting motion within the ITV is sufficient. VMAT/IMRT techniques that treat more conformal target volumes can significantly spare critical OARs such as the carotid arteries and thyroid gland, reducing the risk of cerebrovascular and other long-term complications.

Disclosures

There are no disclosures to declare.

Acknowledgments

This work was done at The Royal Marsden NHS Foundation Trust and The Institute of Cancer Research.

Supplementary materials

Supplementary material associated with this article can be found in the online version at [doi:10.1016/j.adro.2024.101490](https://doi.org/10.1016/j.adro.2024.101490).

References

- Pakkanen P, Irjala H, Ilmarinen T, et al. Survival and larynx preservation in early glottic cancer: A randomized trial comparing laser surgery and radiation therapy. *Int J Radiat Oncol Biol Phys.* 2022;113:96-100.
- Roberts DA, Sandin C, Vesanen PT, et al. Machine QA for the Elekta Unity system: A report from the Elekta MR-linac consortium. *Med Phys.* 2021;48.
- Riis HL, Chick J, Dunlop A, Tilly D. The quality assurance of a 1.5 T MR-Linac. *Semin Radiat Oncol.* 2024;34:120-128.
- Martin JD, Buckley AR, Graeb D, Walman B, Salvian A, Hay JH. Carotid artery stenosis in asymptomatic patients who have received unilateral head-and-neck irradiation. *Int J Radiat Oncol Biol Phys.* 2005;63:1197-1205.
- Petkar I, Rooney K, Roe JWG, et al. DARS: A phase III randomised multicentre study of dysphagia- optimised intensitymodulated radiotherapy (Do-IMRT) versus standard intensity- modulated radiotherapy (S-IMRT) in head and neck cancer. *BMC Cancer.* 2016;16.
- Leonard RJ, Kendall KA, McKenzie S, Gonçalves MI, Walker A. Structural displacements in normal swallowing: A videofluoroscopic study. *Dysphagia.* 2000;15:146-152.
- Hamlet S, Ezzell G, Aref A. Larynx motion associated with swallowing during radiation therapy. *Int J Radiat Oncol Biol Phys.* 1994;28:467-470.
- Van Asselen B, Raaijmakers CPJ, Lagendijk JJW, Terhaard CHJ. Intrafraction motions of the larynx during radiotherapy. *Int J Radiat Oncol Biol Phys.* 2003;56:384-390.
- Bradley JA, Paulson ES, Ahunbay E, Schultz C, Li XA, Wang D. Dynamic MRI analysis of tumor and organ motion during rest and deglutition and margin assessment for radiotherapy of head-and-neck cancer. *Int J Radiat Oncol Biol Phys.* 2011;81.
- Gurney-Champion OJ, McQuaid D, Dunlop A, et al. MRI-based assessment of 3D intrafractional motion of head and neck cancer for radiation therapy. *Int J Radiat Oncol Biol Phys.* 2018;100:306-316.
- Bruijnen T, Stemkens B, Terhaard CHJ, Lagendijk JJW, Raaijmakers CPJ, Tijssen RHN. Intrafraction motion quantification and planning target volume margin determination of head-and-neck tumors using cine magnetic resonance imaging. *Radiother Oncol.* 2019;130:82-88.
- Osman SOS, de Boer HCJ, Heijmen BJM, Levendag PC. Four-dimensional CT analysis of vocal cords mobility for highly focused single vocal cord irradiation. *Radiother Oncol.* 2008;89:19-27.
- Keiper TD, Tai A, Chen X, et al. Feasibility of real-time motion tracking using cine MRI during MR-guided radiation therapy for abdominal targets. *Med Phys.* 2020;47:3554-3566.
- Jassar H, Tai A, Chen X, et al. Real-time motion tracking based on orthogonal cine MRI for abdominal tumors on 1.5T MR-Linac. Paper presented at: AAPM 63rd Annual Meeting and Exhibition. 2021. July 25-29.
- Riede T, Stein A, Baab KL, Hoxworth JM. Post-pubertal developmental trajectories of laryngeal shape and size in humans. *Sci Rep.* 2023;13:7673.
- Hamdan AL, Khalifee E, Ziade G, Semaan S. Sexual dimorphism in laryngeal volumetric measurements using magnetic resonance imaging. *Ear Nose Throat J.* 2020;99:132-136.
- Martin-Harris B, Brodsky MB, Michel Y, Ford CL, Walters B, Heffner J. Breathing and swallowing dynamics across the adult lifespan. *Arch Otolaryngol Head Neck Surg.* 2005;131:762.
- Bahig H, Nguyen-Tan PF, Filion É, et al. Cine-magnetic resonance imaging for assessment of larynx motion in early glottic cancer radiotherapy. MReadings: MR in RT. 2016.
- Boehme S, Bentley AH, Hartmann EK, et al. Influence of inspiration to expiration ratio on cyclic recruitment and derecruitment of atelectasis in a saline lavage model of acute respiratory distress syndrome. *Crit Care Med.* 2015;43:e65-e74.
- Tiong A, Huang SH, O'Sullivan B, et al. Outcome following IMRT for T2 glottic cancer: The potential impact of image-guidance protocols on local control. *J Radiat Oncol.* 2014;3:267-275.
- Gupta A, Dunlop A, Mitchell A, et al. Online adaptive radiotherapy for head and neck cancers on the MR linear Accelerator: Introducing a novel modified Adapt-to-Shape approach. *Clin Transl Radiat Oncol.* 2022;32:48-51.
- McDonald BA, Vedam S, Yang J, et al. Initial Feasibility and clinical implementation of daily MR-guided adaptive head and neck cancer radiation therapy on a 1.5T MR-Linac system: Prospective R-IDEAL 2a/2b systematic clinical evaluation of technical innovation. *Int J Radiat Oncol Biol Phys.* 2021;109:1606-1618.
- Emami D. Tolerance of normal tissue to therapeutic radiation. *Radiother Oncol.* 2013;1:35.
- Rogowski P, von Bestenbostel R, Walter F, et al. Feasibility and early clinical experience of online adaptive mr-guided radiotherapy of liver tumors. *Cancers (Basel).* 2021;13.
- van Timmeren JE, Chamberlain M, Krayenbuehl J, et al. Treatment plan quality during online adaptive re-planning. *Radiat Oncol.* 2020;15:203.
- Huynh E, Boyle S, Campbell J, et al. Technical note: Toward implementation of MR-guided radiation therapy for laryngeal cancer with healthy volunteer imaging and a custom MR-CT larynx phantom. *Med Phys.* 2022;49:1814-1821.
- Green OL, Rankine LJ, Cai B, et al. First clinical implementation of real-time, real anatomy tracking and radiation beam control. *Med Phys.* 2018;45:3728-3740.
- Uijtewaal P, Borman PTS, Woodhead PL, et al. First experimental demonstration of VMAT combined with MLC tracking for single and multi fraction lung SBRT on an MR-linac. *Radiother Oncol.* 2022;174:149-157.